Bioorg. Med. Chem. Lett. 48 (2021) 128249

Contents lists available at ScienceDirect

Bioorganic & Medicinal Chemistry Letters

journal homepage: www.elsevier.com/locate/bmcl

Novel triazole-sulfonamide bearing pyrimidine moieties with carbonic anhydrase inhibitory action: Design, synthesis, computational and enzyme inhibition studies

Shoaib Manzoor [a], Andrea Petreni [b], Md Kausar Raza [c], Claudiu T. Supuran [b,*], Nasimul Hoda [a,*]

[a] Drug Design and Synthesis Laboratory, Department of Chemistry, Jamia Millia Islamia, New Delhi 110025, India
[b] University of Florence, Department of Neuroscience Psychology, Drug Research and Child's Health, Section of Pharmaceutical and Nutraceutical Sciences, Via Ugo Schiff 6, 50019 Sesto Fiorentino, Italy
[c] Department of Inorganic and Physical Chemistry, Indian Institute of Science, Bangalore 560012, India

ARTICLE INFO

Keywords:
Triazole
Pyrimidine
Sulfonamide
Carbonic anhydrase inhibitors
Docking

ABSTRACT

A series of new triazole-sulfonamide bearing pyrimidine derivatives were designed and synthesized via click chemistry. All new compounds (**SH-1** to **SH-28**) were validated by ^{1}HNMR, ^{13}CNMR, HRMS, and **SH-3** was further structurally validated by X-Ray single diffraction study. These compounds (**SH-1** to **SH-28**) were tested as inhibitors of human carbonic anhydrase (*h*CA) isoforms, such as *h*CA I, II, IX and XII, using a stopped flow CO_2 hydrase assay. Most of the compounds exhibited significant inhibitory activity against *h*CA II and weak inhibitory activity against *h*CA I. The target compounds also displayed moderate to excellent inhibitory activity against tumor-related *h*CAs IX and XII. Some compounds, e.g., **SH-20** (K_i = 9.4 nM), **SH-26** (K_i = 1.8 nM) and **SH-28** (K_i = 0.82 nM) exhibited excellent inhibitory activity and selectivity profile against *h*CAs XII over IX. **SH-23** displayed promising inhibitory activity and selectivity profile against both tumor-related *h*CAs IX (K_i = 2.9 nM) as well as XII (K_i = 0.82 nM) over *h*CA I and II. To understand the molecular interactions, molecular docking study of compounds **SH-20**, **SH-23**, **SH-26** and **SH-28** with *h*CA XII and **SH-23** also with *h*CA IX were performed. The computational study evidenced favorable interaction between the inhibitors and active residues of both proteins. Some of these derivatives are promising leads for the development of selective, anticancer agents based on CA inhibitors.

Introduction

Carbonic anhydrases (CAs, EC 4.2.1.1) found in all organisms are a superfamily of zinc metalloenzymes which catalyzes the reversible hydration of CO_2 and H_2O to HCO_3^- and H^+ ions ($CO_2 + H_2O \rightleftharpoons HCO_3^- + H^+$). Currently, 15 different isoforms of CA in humans have been discovered and these isoforms have different subcellular localizations, among which *h*CA I-III, VII and XIII are cytosolic, *h*CA IV, IX, XII, and XIV are membrane bound, *h*CA VA and VB are mitochondrial, isoform VI is secreted whereas the CA isoforms VIII, X and XI are acatalytic. Through any of these CA isoforms, cells can easily regulate the extracellular and intracellular pH and CO_2/HCO_3^- pools[1–8]. The distribution of human CA isoforms varies from one isoform to another, with some isoforms being particularly abundant in most cells and tissues (e.g., CA I, CA II), whereas CA IV is particularly abundant in kidneys, lungs, and ciliary processes of eye. Other isoforms have a comparatively restricted tissue distribution e.g., CA IX, in normal physiologic conditions, is mainly found in the epithelium lining the stomach and small intestines[1,9]. CAs plays a key role in various pathological conditions and currently the investigation of CA inhibition is a very active research area taking account of the presence of multiple isoforms of this enzyme. In various pathological conditions CAs were identified to play crucial roles, for example in some central nervous system (CNS) diseases, glaucoma, cancer, and obesity[1,10–12]. In recent years, *h*CA IX and XII became fascinating targets for the discovery of new anti-proliferative compounds, due to their significant role in the survival, proliferation and spread of cancer cells. In hypoxic conditions, *h*CA IX and *h*CA XII participate in the regulation of extracellular and intracellular pH as well as the metabolism of the tumor cell, and therefore, their selective inhibition triggers interesting antitumor clinical effects[12–13].

* Corresponding authors.
E-mail addresses: shoaibchem19@gmail.com (S. Manzoor), claudiu.supuran@unifi.it (C.T. Supuran), nhoda@jmi.ac.in (N. Hoda).

https://doi.org/10.1016/j.bmcl.2021.128249
Received 5 May 2021; Received in revised form 26 June 2021; Accepted 1 July 2021
Available online 6 July 2021
0960-894X/

The primary sulfonamide scaffold plays a significant role in CA inhibition, being among the versatile scaffolds used to build up selective and potent CA inhibitors[1–2,14–17]. Currently, >30 sulfonamide-based compounds are in clinical use with few examples such as acetazolamide (AAZ) A, methazolamide B, ethoxzolamide C, celecoxib D[4], dichlorophenamide E, dorzolamide F (Fig. 1). In deprotonated form, the sulfonamide derivatives bind to CAs at the active site zinc (II) ion through the primary nitrogen atom of the sulfonamide moiety. Depending upon the modifications of the sulfonamide scaffolds, additional interactions with hydrophilic and hydrophobic amino acids residues occur within the CA active site. Therefore, novel CA inhibitors can be designed and synthesized using the benzenesulfonamide as head groups by incorporating a variety of substitution patterns on these scaffolds and on their tails[10,18–21].

Click chemistry has been widely used to achieve CA inhibitors belonging to the sulfonamide class. Copper-catalyzed azide−alkyne cycloadditions (CuAAC) have achieved a significant role due to their short reaction time, good yields, and their modularity[21–25]. Triazole-sulfonamide scaffolds incorporating substituted aromatic aryl or heterocyclic groups by means of uncleavable flexible linkers of the ether (CH_2O–), or amine (CH_2NH) types led obtained to effective CA inhibitors[26].

For the design of new CA inhibitors, in the present work the triazole-sulfonamide scaffold was fused with substituted pyrimidine rings through linkers of the CH_2O– type, for enhancing the flexibility, which may produce significant interaction within the CA active sites, as well as selectivity profiles for the various isoforms (Fig. 2). The increasing flexibility of inhibitors may increase degrees of freedom and decrease molecular tension, whereas aromatic tails can improve the interaction with favorable sub pocket of the enzymes[27]. The incorporation of substituted pyrimidine ring as tails to classical benezenesulfonamide scaffolds was investigated, in order to assure effective binding with various CA isoenzymes. The pyrimidine hybrids are the most common nitrogen based heterocycle in nature and are associated in various cellular and metabolic processes[28–30]. Pyrimidine like hybrids have been developed that exhibit potential anti-tumor and anti-neurodegenerative activity[31–33]. Pyrimidine derivatives were shown to inhibit cytosolic *h*CA I, *h*CA II, *h*CA IV and *h*CA IX, which may be of interest for the development of tighter-binding inhibitors[34–35].

Hence, we reported a new series of triazole-sulfonamide based pyrimidine derivatives, that were designed, synthesized, and tested for their inhibitory activity against *h*CA I, II, IX and XII. It was expected that the introduction of substituted pyrimidine as a tail along with ether (CH_2O–) linker will give better flexibility for inhibition of CAs.

The synthesis of triazole-sulfonamide based pyrimidine derivatives (**SH-1** to **SH-28**) is shown in scheme 1 and 2. The new derivatives (**SH-1** to **SH-28**) were synthesized from commercially available benzenesulfonamide. As shown in Scheme 1, two distinct synthetic methods were used to obtain 2,4-dichloropyrimidine derivatives **5** (**a** and **b**). 2,4-dichloro pyrimidine **5a** was obtained from commercially available uracil (**4a**) refluxed in $POCl_3$. 2,4-dichloro-6-methylpyrimidine (**5b**) was obtained in multiple steps as shown in scheme 1. The ethyl acetoacetate (1) and thiourea (2) were reacted in water in presence of K_2CO_3 and conc. HCl to give 6-methyl-2-thioxo-2,3-dihydropyrimidin-4(1H)-one **(3)**. 6-methyluracil **(4)** was obtained from 6-methyl-2-thioxo-2,3-dihydropyrimidin-4(1H)-one **(3)** refluxed in chloroacetic acid and water in presence of HCl. 6-methyluracil **(4b)** was refluxed in $POCl_3$ to obtain 2,4-dichloro-6-methylpyrimidine (**5b**). Both 2,4-dichloropyrimidines **5(a** and **b)** were reacted with propargyl alcohol in DMF to obtain intermediates **6 (a** and **b)** in presence of K_2CO_3 as a base.

As shown in scheme 2, benzenesulfonamide azide (**8**) was obtained from commercially available benzenesulfonamide (**7**). The intermediate triazole-benzenesulfonamide pyrimidine **9** (**a** and **b**) were synthesized by click chemistry from intermediate **6(a** and **b)** and freshly prepared benzenesulfonamide azides (**8**) in the presence of $CuSO_4{\cdot}5H_2O$ and sodium ascorbate. The intermediate triazole-benzenesulfonamide pyrimidine **9(a** and **b)** was reacted in dry DMF with different substituted secondary amines using K_2CO_3 as base, affording the target triazole-sulfonamide based pyrimidine derivatives (**SH-1** to **SH-28**). The synthesized compounds were purified by using flash column chromatography. The target compounds (**SH-1** to **SH-28)** were well validated by using mass spectroscopy, ^1H and ^{13}C nuclear magnetic resonance (NMR) and **SH-3** was further structurally validated by X-Ray single diffraction study. The purity of the all the final compounds was analyzed by UPLC (Ultra Performance Liquid Chromatography) and was > 94%.

Compound **SH-3** was structurally characterized by single crystal X-ray crystallography (Fig. 3 and Table 1 and **Figs. S85 and S86, supporting information**). The **SH-3** compound crystallized in P121/c1 space group of the monoclinic system. In unit-cell packing diagram of **SH-3** compound exhibited the hydrogen bonding interaction between the hydrogen atom of the sulfamoyl (N-7) and the ethereal oxygen (O-1) at a distance of 2.436 Å. The hydrogen of pyrimidine at C-9 also displayed the hydrogen bonding interaction with oxygen atoms of sulfamoyl group at a distance of 2.367 Å. The unit cell packing diagrams of **SH-3** showed short contact bonding with their adjacent atoms. The unit cell packing diagram of **SH-3** compound are given in supporting

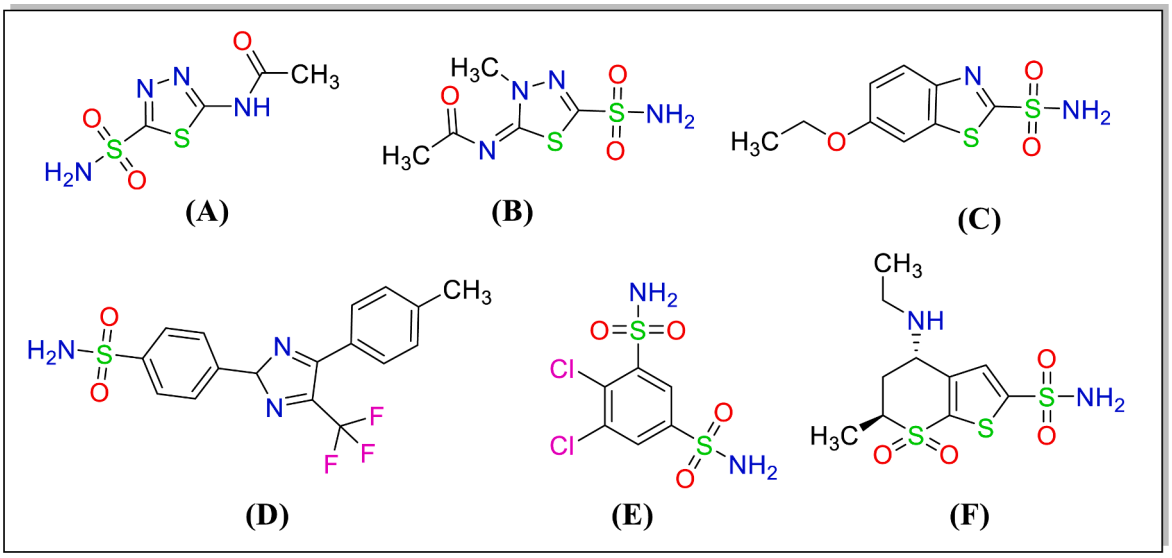

Fig. 1. Clinically used sulfonamide-based CA inhibitors **A-F**.

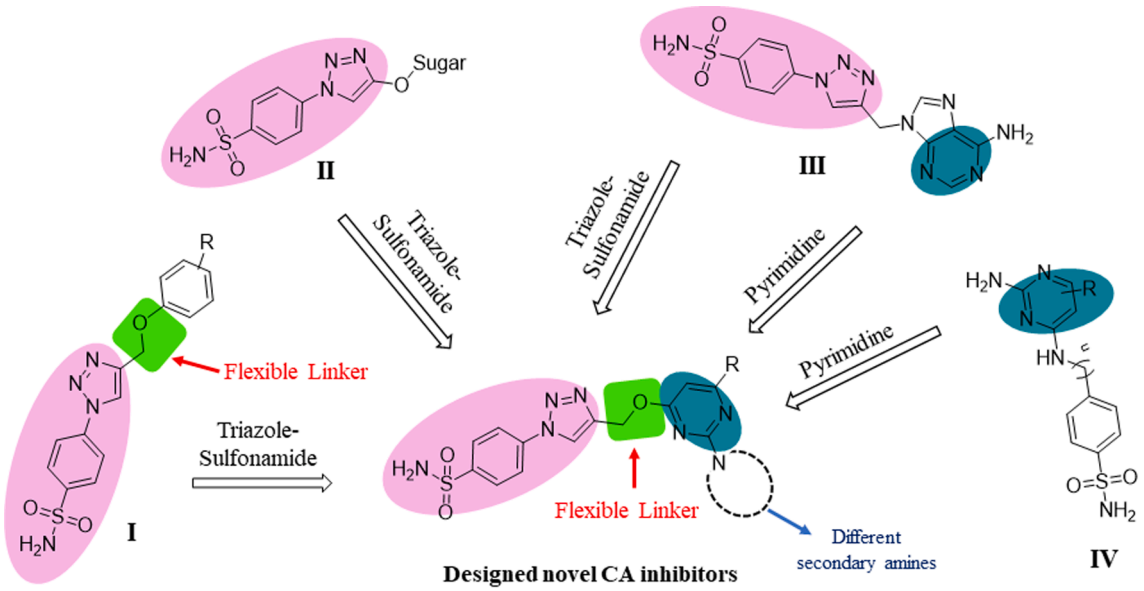

Fig. 2. Design strategy of novel CA inhibitors.

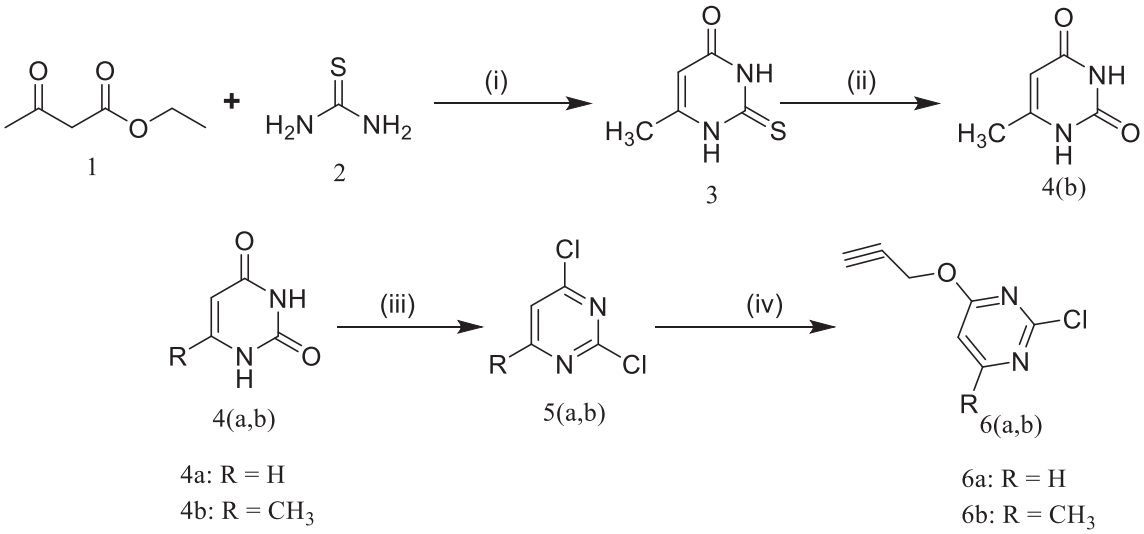

Scheme 1. Reagents and conditions: (i) H_2O, K_2CO_3, Conc. HCl, 100 °C; **(ii)** Chloroacetic acid, water, conc. HCl, reflux; (iii) $POCl_3$, Reflux, 3–4 h; (iv) propargyl alcohol, K_2CO_3, DMF, 60–70 °C, N_2.

information (**Figs. S85 and S86, Supporting information**).

The synthesized new triazole-sulfonamide linked with pyrimidine derivatives **(SH-1** to **SH-28)** were assessed for their inhibition potential against four human CA isoforms, namely, the cytosolic isoforms, *h*CA I and *h*CA II and the *trans*-membrane tumor-related isoforms, *h*CA IX and *h*CA XII, by a stopped flow CO_2 hydrase assay method using acetazolamide as standard drug. The following structure−activity relationship (SAR) were highlighted from CA inhibition data of Table 2.

1. *h*CA I: All the synthesized compounds (**SH-1 to SH-28**) against ubiquitous cytosolic *h*CA I displayed inhibitory activity between nanomolar range (K_i = 41.5 to 94.8 nM) to micromolar range (K_i = 181.8 to 6745 nM). The compounds morpholine (**SH-1**), piperidine (**SH-3**) and ethyl piperazine-1-carboxylate (**SH-12**) bearing sulfamoylphenyl-pyrimidine and *N*-methylpiperazine (**SH-16**) and ethyl piperazine-1-carboxylate (**SH-26**) bearing sulfamoylphenyl-6-methylpyrimidine displayed satisfactory inhibition toward hCA I with K_i value ranging from 61.9 to 94.8 nM. However, the derivatives contain *N*-methylpiperazine (**SH-2**) linked with sulfamoylphenyl-pyrimidine and *N*-ethylpiperazine (**SH-19**) with sulfamoylphenyl-6-methylpyrimidine displayed significant inhibitory activity towards *h*CA I with K_i value 41.5 and 44.3 nM respectively. Moreover, the rest of the compounds showed weak inhibitions against *h*CA I.
2. *h*CA II: Most of the synthesized compounds showed effective inhibitory activity against *h*CA II isoform (K_i values ranging from 0.31 to 34.1 nM). However, derivatives which contain *p*-methoxyphenylpiperazine (**SH-6**) and 2-piperazinylpyridine (**SH-10**) linked with sulfamoylphenyl-pyrimidine and 2-piperazin-1-ylnicotinonitrile (**SH-18**) and *p*-chlorobenzylpiperazine (**SH-23**) with sulfamoylphenyl-6-methylpyrimidine showed satisfactory inhibitory activity between nanomolar range (K_i = 13.5 to 34.1 nM), which are slightly weaker inhibitors compared to the AAZ standard drug (K_i = 12.0 nM). While the rest of the compounds showed strong inhibitions against *h*CA II. It is noteworthy that few compounds were found to act as subnanomolar *h*CA II inhibitors, e.g., **SH-7** (K_i = 0.59 nM), **SH-11** (K_i = 0.80 nM), **SH-13** (K_i = 0.65 nM), **SH-22** (K_i = 0.92 nM) and

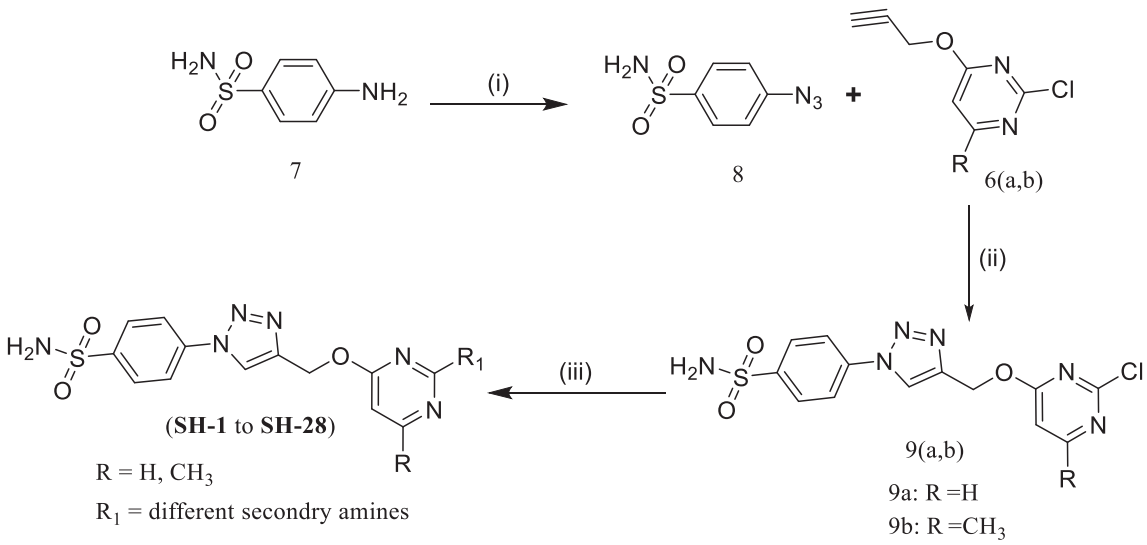

Scheme 2. Reagents and conditions: (i) $NaNO_2$, HCl 6 N; NaN_3, 2 h, rt, 100 °C; **(ii)** $CuSO_4{\cdot}5H_2O$, sodium ascorbate, H_2O:THF, 50–60 °C, 3 h; (iii) different secondary amines, K_2CO_3, DMF, 3–4 h, 70–80 °C.

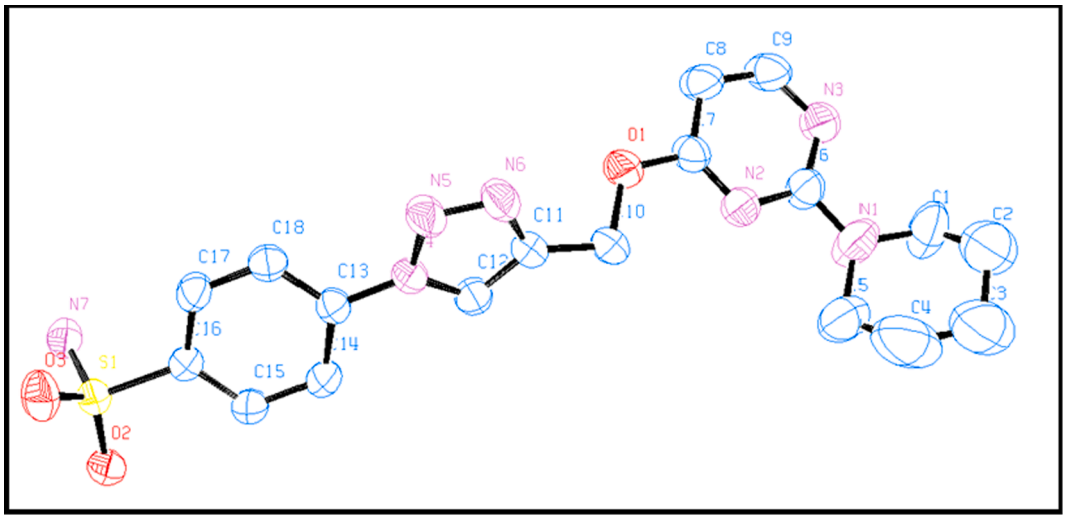

Fig. 3. ORTEP diagram of compounds **SH-3** (50% probability level of thermal ellipsoids). Color codes: Carbon, light blue; Nitrogen: lavender; Oxygen: red and S, light yellow. Hydrogen atoms are hidden for clarity.

SH-27 (K_i = 0.83 nM). The compounds benzylpiperazine and *o*-methoxyphenylpiperazine bearing sulfamoylphenyl-pyrimidine were found to acts as promising *h*CA II inhibitors at low nanomolar range, e.g., **SH-8** (K_i = 1.4 nM) and **SH-14** (K_i = 1.2 nM).

3. *h*CA IX: The tumor-related isoform *h*CA IX was inhibited by all the synthesized compounds (**SH-1** to **SH-28**) in the 1.6–465.7 nM range. Derivatives which contain ethyl piperazine-1-carboxylate **(SH-12)** with sulfamoylphenyl-pyrimidine and *p*-chlorobenzylpiperazine **(SH-23)** and 2-piperazinylpyridine **(SH-24)** with sulfamoylphenyl-6-methylpyrimidine displayed strong inhibitory activity against *h*CA IX. Interestingly, *p*-chlorobenzylpiperazine substituted derivative **SH-23** appeared as an excellent *h*CA IX inhibitor, along with high selectivity towards *h*CA I and *h*CA II. Derivative **SH-23** displayed > 299-fold selectivity over hCA I and > 11-fold selectivity over hCA II. Compounds **SH-2**, **SH-9**, **SH-11**, **SH-13**, **SH-15**, **SH-16**, **SH-18**, **SH-20**, **SH-25**, and **SH-26** displayed nearly the same inhibition (24.1–33.4 nM) of *h*CA IX to that of the standard drug AZZ (25.0 nM). Only three derivatives, 2-piperazin-1-ylnicotinonitrile **(SH-4)**, bulkier diphenyl-piperazine (**SH-7)** in series I and *p*-fluorophenylpiperazine (**SH-27)** in series II, with K_i values 155.2, 192.0 and 465.7 nM respectively displayed weaker inhibitory activity against *h*CA IX.
4. *h*CA XII: Most of the compounds displayed significant inhibitory activity against tumor-related *h*CA XII isoform with K_i values ranging from 0.36 to 90.5 nM. However, Compounds **SH-3**, **SH-4**, **SH-5**, **SH-12**, **SH-15**, **SH-16**, **SH-19**, **SH-23**, **SH-26**, and **SH-28** showed effective inhibitory potency in the subnanomolar range (0.36 to 0.90 nM) against *h*CA XII isoform as compared to AAZ standard drug (5.7 nM). Derivatives which contain *p*-methoxyphenylpiperazine (**SH-20)**, *o*-methoxyphenylpiperazine (**SH-28)**, and ethyl piperazine-1-carboxylate (**SH-26)** with sulfamoylphenyl-6-methylpyrimidine displayed as significant *h*CA XII inhibitors. The compounds **SH-20** was 16-fold, **SH-26** was 37-fold and **SH-28** was 44-fold more selective against tumor-related *h*CA XII isoform than tumor-related *h*CA IX isoform. Moreover, the *p*-chlorobenzylpiperazine substituted derivative **SH-23** displayed promising *h*CA XII inhibitor, which possessed subnanomolar activity (0.82 nM) along with significant selectivity towards *h*CA I and *h*CA II. Derivative **SH-23** showed 1057-fold selectivity over *h*CA I and > 41-fold selectivity over *h*CA II. In addition, compounds **SH-6**, **SH-10 and SH-25** showed satisfactory

Table 1
Selected crystal data and structure refinement for ***4-(4-(((2-(piperidin-1-yl) pyrimidin-4-yl)oxy)methyl)-1H-1,2,3-triazol-1-yl)benzenesulfonamide*** **(SH-3).**

	SH-3
Empirical formula	$C_{36}H_{42}N_{14}O_6S_2$
Fw/g M^{-1}	415.16
Crystal system	monoclinic
Space group	P121/c1
a/Å	8.748(9)
b/Å	10.2760(10)
c/Å	16.4122(15)
***α*/°**	90
***β*/°**	106.155(3)
***γ*/°**	90
V/Å^3	2237.3(4)
Z	2
T, K	298(2)
ρ_{calcd}/Mg m^{-3}	1.233
λ/Å (Mo-Kα)	0.71073 Å
Data/restraints/param	3937/9/270
F(000)	872
GOF	1.107
R(F_o),[a] I > 2 σ(I) [w*R*(F_o)[b]]	0.0595 [0.1665]
R (all data) [w*R* (all data)]	0.0825 [0.1772]
Largest diff peak, hole (e Å^{-3}	0.431, −0.420
w = 1/[(σF_o)^2 + (AP)^2 + (BP)]	A = 0.1020B = 0.3210

[a] $R = \sum iF_oi - iF_cii/\sum iF_oi$
[b] $wR = \{\sum[w(F_o^2 - F_c^{22}]/\sum[w(F_o)^2]\}^{1/2}$, where $P = (F_o^2 + 2F_c^2/3$.

inhibitory activity in the nanomolar range (K_i = 7.4–9.5 nM), which are slightly weaker inhibitors compared to the AAZ standard drug. Compounds **SH-1**, **SH-2**, **SH-7**, **SH-9**, **SH-11**, **SH-13**, **SH-14**, **SH-18**, **SH-21**, and **SH-27** displayed weaker inhibitory activity against *h*CA XII with K_i values ranging from 38.4 to 78.9 nM.

It is clearly evoked by SAR study that the ether linker containing triazole sulfamoylphenyl based pyrimidine derivatives showed significant activity towards tumor-related *h*CAs IX and XII. The most active compounds **SH-20**, **SH-26** and **SH-28** bestowed significant inhibition for *h*CA XII isoform. In addition, **SH-23** displayed excellent inhibition for both *h*CA IX as well as *h*CA XII.

In this study, a molecular docking study was performed to analyze the interaction of some of the new sulfonamides within the active site of *h*CA IX and *h*CA XII, for rationalizing the drug-receptor interaction. However, binding free energy and interaction of the best posed compounds were investigated by AutoDock vina program. In our study, compounds **SH-20**, **SH-26** and **SH-28** showed significant selectivity towards *h*CA XII, and **SH-23** exhibited significant selectivity towards both *h*CA IX and *h*CA XII, was taken account for this study. The compounds **SH-20**, **SH-26** and **SH-28** were thus docked into *h*CA XII and **SH-23** were docked into *h*CA IX and *h*CA XII using AutoDock vina software 1.5.7 (Figs. 4 and 5**).** The molecular docking study revealed that these triazole-sulfonamide based pyrimidine compounds displayed higher binding affinity towards *h*CA IX and *h*CA XII and benzenesulfonamide moiety accommodates exactly into the active catalytic pocket towards zinc ion.

It has been found that compounds **SH-20**, **SH-26** and **SH-28** has best scores with −8.4, −7.6 and −8.7 kcal/mol towards *h*CA XII, respectively. The compounds are stabilized by hydrogen bond interaction between the –NH of sulfonamide with Thr199 amino acid residue in Fig. 4 (**A**, **B** and **C**). These compounds are further stabilized by hydrogen bond interaction between sulfonamide oxygen with the peptide –NH of Thr199 and Thr200 residues. The nitrogen rich triazole moiety of the **SH-20** (Fig. 4**A**), **SH-26** (Fig. 4**B**) and **SH-28** (Fig. 4**C**) compounds formed a short contacting hydrogen bond with Asn62, Lys67 and Gln92 residues in *h*CA XII. The tail portion (piperazine based derivatives) exhibited van der walls interaction with the residues Thr91, Ala131 and Ser132, which might involve in selectivity of compounds towards *h*CA

Table 2
Inhibition data of human hCA isoforms **I**, **II**, **IX** and **XII** for compounds **SH-1** to **SH-28** using as **AAZ** standard drug.

Compd	R	R_1	K_i (nM)[a]			
			hCA I	hCA II	hCA IX	hCA XII
SH-1	H		81.7	0.43	42.5	78.9
SH-2	H		41.5	0.63	30.4	90.5
SH-3	H		89.6	0.31	41.3	0.81
SH-4	H		628.9	0.66	155.2	0.87
SH-5	H		6173	0.86	22.7	0.71
SH-6	H		830.9	13.5	51.4	9.4
SH-7	H		563.4	0.59	192.0	78.8
SH-8	H		315.0	1.4	39.1	5.3
SH-9	H		6745	9.1	32.2	66.6
SH-10	H		845.8	16.8	16.8	9.5
SH-11	H		441.3	0.80	26.3	70.7
SH-12	H		85.4	3.4	1.6	0.76
SH-13	H		1610	0.65	25.8	48.8
SH-14	H		243.6	1.2	44.7	64.4
SH-15	CH_3		181.8	0.87	30.2	0.69
SH-16	CH_3		61.9	0.61	24.1	0.36
SH-17	CH_3		737.3	6.5	35.8	23.6
SH-18	CH_3		2324	28.5	32.0	68.9
SH-19	CH_3		44.3	0.32	16.1	0.55
SH-20	CH_3		866.7	4.7	29.7	1.8
SH-21	CH_3		4646	8.5	21.4	38.4
SH-22	CH_3		391.4	0.92	41.1	22.0
SH-23	CH_3		867.4	34.1	2.9	0.82
SH-24	CH_3		652.7	7.1	9.1	5.6
SH-25	CH_3		5583	3.7	32.8	7.4
SH-26	CH_3		94.8	3.9	33.4	0.90
SH-27	CH_3		3254	0.83	465.7	47.4
SH-28	CH_3		428.3	4.0	36.3	0.82
AAZ			250.0	12.0	25.0	5.7

[a] Mean from 3 different assays, by a stopped flow technique (errors were in the range of ± 5–10% of the reported values).

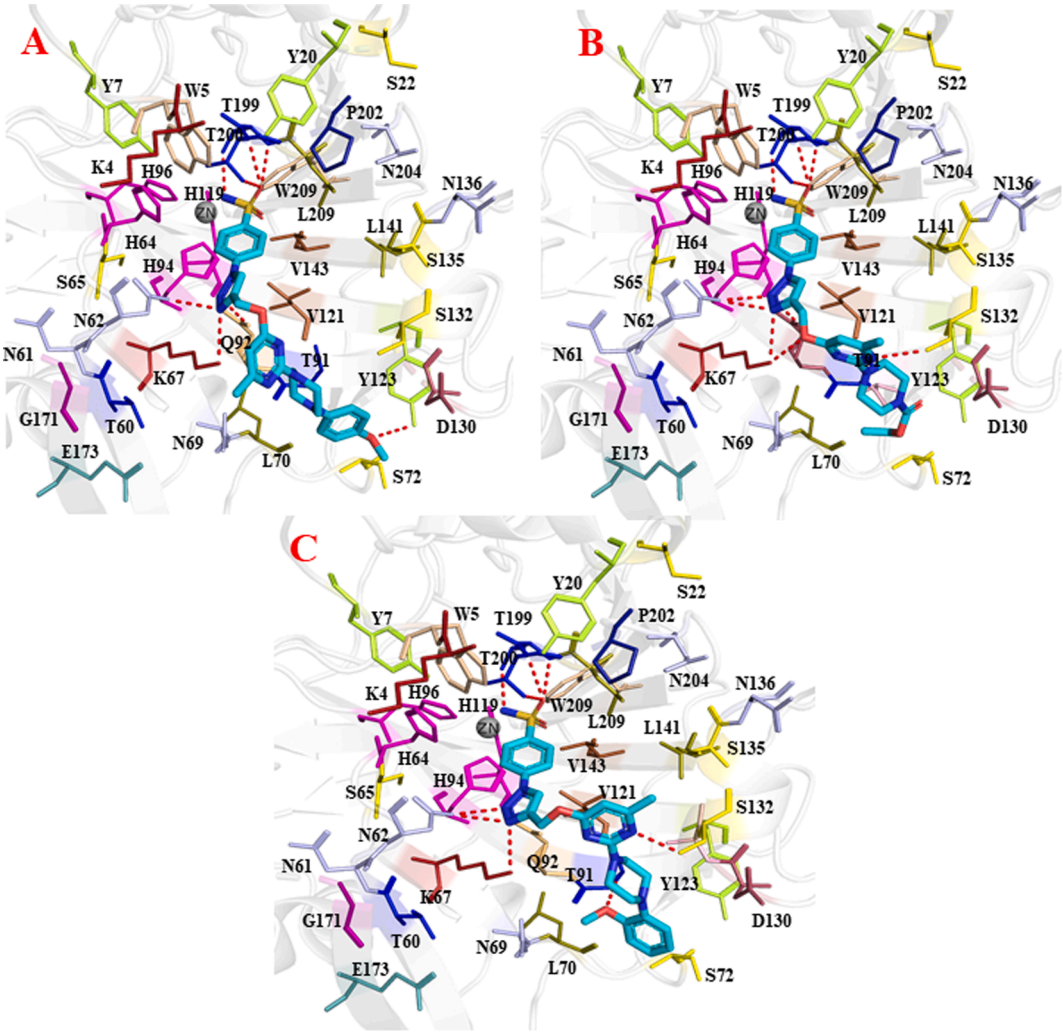

Fig. 4. Compound **SH-20** (A), **SH-26** (B), **SH-28** (C) best docking pose in *h*CA XII (pdb: **1JDO**).

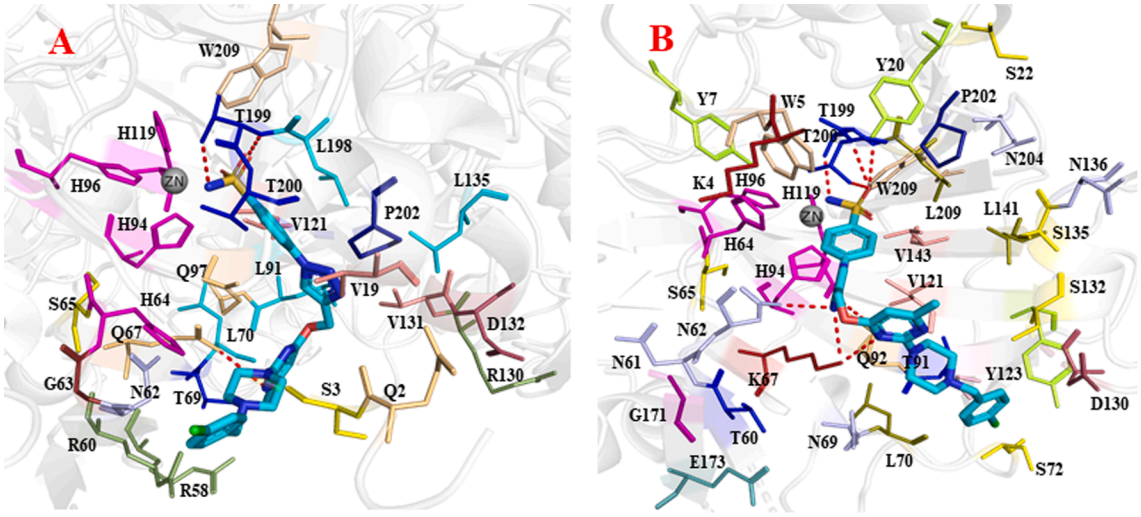

Fig. 5. (A) Compound **SH-23** best docking pose in *h*CA IX (pdb: **3IAI**); (B) Compound **SH-23** best docking pose in *h*CA XII (pdb:**1JDO**).

XII. In addition, oxygen of methoxy group of **SH-20** and carbonyl oxygen group of **SH-28** displayed hydrogen bond with Tyr123 and Thr91 residues in *h*CA XII respectively and nitrogen of pyrimidine moiety of **SH-26** also exhibited hydrogen bond with Ser132.

Similarly, **SH-23** has best scores with −7.1 and −8.2 kcal/mol towards *h*CA IX and *h*CA XII, respectively. The compound **SH-23** is stabilized by hydrogen bond interaction between the –NH of sulfonamide with Thr199 residue in *h*CA IX and *h*CA XII in Fig. 5 **(A and B)**. The **SH-**

23 compound is further stabilized by hydrogen bond interaction between sulfonamide oxygen with the peptide –NH of Thr199 in *h*CA IX and with Thr199 and Thr200 in *h*CA XII. The electron rich pyrimidine moiety of the **SH-23** in *h*CA IX displayed hydrogen bond interaction with Leu70 side chain (Fig. 5**A)** and triazole moiety of **SH-23** in *h*CA XII also formed hydrogen bonds with Asn62, Lys67 and Gln92 residues (Fig. 5**B)**. Therefore, docking study confirms the importance of triazole and pyrimidine derivatives in generating selective and potency between CA enzymes.

In summary, a series of new designed triazole-sulfonamide bearing pyrimidine derivatives were synthesized via click chemistry. All the synthesized compounds (**SH-1** to **SH-28**) were validated by ^{1}HNMR, ^{13}CNMR, HRMS, and **SH-3** was structurally validated by X-Ray single diffraction analysis. The target compounds (**SH-1** to **SH-28**) were tested on *h*CA isoforms like *h*CA I, II, IX and XII, using a stopped flow CO_2 hydrase assay. Most of the compounds displayed poor inhibitory activity against *h*CA I (K_i 41.5 to 5583 nM) and significant inhibitory activity towards hCA II (K_i 0.31 to 34.1 nM). The compounds also show moderate to excellent inhibitory activity against tumor-related *h*CAs IX (K_i 1.6 to 465.7 nM) and CA XII (K_i 0.36 to 90.5 nM). Among all compounds, **SH-20**, **SH-26** and **SH-28** compounds exhibited significant inhibitory activity and selectivity profile against the tumor-related *h*CA XII. However, **SH-20** was 16-fold, **SH-26** was 37-fold and **SH-28** was 44-fold more selective against *h*CA XII than *h*CA IX. In addition, **SH-23** displayed excellent inhibitory activity and selectivity profile against both tumor-related *h*CAs IX (K_i 2.9 nM) as well as XII (K_i 0.82 nM) over *h*CA I and *h*CA II. Molecular docking study of **SH-20**, **SH-23**, **SH-26** and **SH-28** with *h*CA XII and **SH-23** with *h*CA IX were performed by AutoDock Vina, and their binding modes signifies their significant interaction with active residues of protein. The docking study implies that benzenesulfonamide moiety accommodates exactly into the active catalytic pocket towards zinc ion of CA. These results revealed that these triazole-sulfonamide based pyrimidine compounds displayed higher binding affinity towards *h*CA IX and *h*CA XII. Therefore, these derivatives **SH-20**, **SH-23**, **SH-26** and **SH-28** could be promising leads for the development of selective and potential inhibitors as anticancer agents.

Declaration of Competing Interest

The authors declare that they have no known competing financial interests or personal relationships that could have appeared to influence the work reported in this paper.

Acknowledgments

Shoaib Manzoor (S. M.) is extremely thankful to University Grants Commission, Government of India for financial assistance through Central University Ph.D. Students Fellowship.

Appendix A. Supplementary data

Supplementary data to this article can be found online at https://doi.org/10.1016/j.bmcl.2021.128249.

References

[1] Supuran CT. Carbonic anhydrases: novel therapeutic applications for inhibitors and activators. *Nat Rev Drug Discov*. 2008;7(2):168–181. https://doi.org/10.1038/nrd2467.
[2] Alterio V, Di Fiore A, D'Ambrosio K, Supuran CT, De Simone G. Multiple Binding Modes of Inhibitors to Carbonic Anhydrases: How to Design Specific Drugs Targeting 15 Different Isoforms? *Chem Rev*. 2012;112:4421–4468. https://doi.org/10.1021/cr200176r.
[3] Smeulders MJ, Barends TRM, Pol A, et al. Evolution of a new enzyme for carbon disulphide conversion by an acidothermophilic archaeon. *Nature*. 2011;478(7369):412–416. https://doi.org/10.1038/nature10464.
[4] Rummer JL, McKenzie DJ, Innocenti A, Supuran CT, Brauner CJ. Root Effect Hemoglobin May Have Evolved to Enhance General Tissue Oxygen Delivery. *Science*. 2013;340(6138):1327–1329. https://doi.org/10.1126/science:1233692.
[5] Supuran CT. Carbonic anhydrases: from biomedical applications of the inhibitors and activators to biotechnological use for CO2 capture. *J Enzyme Inhib Med Chem*. 2013;28:229–230. https://doi.org/10.3109/14756366.2013.761876.
[6] Neri D, Supuran CT. Interfering with pH regulation in tumours as a therapeutic strategy. *Nat. Rev. Drug Discov*. 2011;10(10):767–777. https://doi.org/10.1038/nrd3554.
[7] Smith KS, Jakubzick C, Whittam TS, Ferry JG. Carbonic anhydrase is an ancient enzyme widespread in prokaryotes. *Proc Natl Acad Sci*. 1999;96(26):15184–15189. https://doi.org/10.1073/pnas.96.26.15184.
[8] Supuran CT. Structure-based drug discovery of carbonic anhydrase inhibitors. *J Enzyme Inhib Med Chem*. 2012;27(6):759–772. https://doi.org/10.3109/14756366.2012.672983.
[9] Zamanova S, Shabana AM, Mondal UK, Ilies MA. Carbonic anhydrases as disease markers. *Expert Opin Ther Pat*. 2019;29(7):509–533. https://doi.org/10.1080/13543776.2019.1629419.
[10] Supuran CT. How many carbonic anhydrase inhibition mechanisms exist? *J Enzyme Inhib Med Chem*. 2016;31(3):345–360. https://doi.org/10.3109/14756366.2015.1122001.
[11] Supuran CT. Applications of carbonic anhydrases inhibitors in renal and central nervous system diseases. *Expert Opin Ther Pat*. 2018;28(10):713–721. https://doi.org/10.1080/13543776.2018.1519023.
[12] Cakmak EB, Zengin Kurt B, Ozturk Civelek D, et al. Quinoline-sulfamoyl carbamates/sulfamide derivatives: Synthesis, cytotoxicity, carbonic anhydrase activity, and molecular modelling studies. *Bioorg Chem*. 2021;110, 104778. https://doi.org/10.1016/j.bioorg.2021.104778.
[13] Pastorekova, S. Parkkila, S. Zavada, J. Tumor-associated Carbonic Anhydrases and Their Clinical Significance, in: 2006: pp. 167–216. 10.1016/S0065-2423(06)42005-9.
[14] Morsy SMI, Badawi AM, Cecchi A, Scozzafava A, Supuran CT. Carbonic anhydrase inhibitors. Biphenylsulfonamides with inhibitory action towards the transmembrane, tumor-associated isozymes IX possess cytotoxic activity against human colon, lung and breast cancer cell lines. *J Enzyme Inhib Med Chem*. 2009;24(2):499–505. https://doi.org/10.1080/14756360802218441.
[15] Krishnamurthy VM, Kaufman GK, Urbach AR, et al. Carbonic Anhydrase as a Model for Biophysical and Physical-Organic Studies of Proteins and Protein−Ligand Binding. *Chem Rev*. 2008;108(3):946–1051. https://doi.org/10.1021/cr050262p.
[16] McKenna, R. Carbonic Anhydrase: Its Inhibitors and Activators. CRC Enzyme Inhibitors Series, Volume 1 Edited by Claudiu T. Supuran, Andrea Scozzafava (Universita degli Studi, Firenze), and Janet Conway (Pfizer Inc., New York). CRC Press LLC: Boca Raton, FL. 2004. xii, J Am Chem Soc 127; 2005, 3643–3643. 10.1021/ja040999g.
[17] Abdelrahman MA, Ibrahim HS, Nocentini A, et al. Novel 3-substituted coumarins as selective human carbonic anhydrase IX and XII inhibitors: Synthesis, biological and molecular dynamics analysis. *Eur J Med Chem*. 2021;209, 112897. https://doi.org/10.1016/j.ejmech.2020.112897.
[18] Zubrienė A, Čapkauskaitė E, Gylytė J, Kišonaitė M, Tumkevičius S, Matulis D. Benzenesulfonamides with benzimidazole moieties as inhibitors of carbonic anhydrases I, II, VII, XII and XIII. *J Enzyme Inhib Med Chem*. 2014;29(1):124–131. https://doi.org/10.3109/14756366.2012.757223.
[19] De Simone G, Monti SM, Alterio V, et al. Crystal structure of the most catalytically effective carbonic anhydrase enzyme known, SazCA from the thermophilic bacterium Sulfurihydrogenibium azorense. *Bioorg Med Chem Lett*. 2015;25(9):2002–2006. https://doi.org/10.1016/j.bmcl.2015.02.068.
[20] Fisher SZ, Govindasamy L, Boyle N, et al. X-ray crystallographic studies reveal that the incorporation of spacer groups in carbonic anhydrase inhibitors causes alternate binding modes. *Acta Crystallogr Sect F Struct Biol Cryst Commun*. 2006;62(7):618–622. https://doi.org/10.1107/S1744309106020446.
[21] Di Fiore A, Capasso C, De Luca V, et al. X-ray structure of the first 'extremo-α-carbonic anhydrase', a dimeric enzyme from the thermophilic bacterium Sulfurihydrogenibium yellowstonense YO3AOP1. *Acta Crystallogr D Biol Crystallogr*. 2013;69(6):1150–1159. https://doi.org/10.1107/S0907444913007208.
[22] Mocharla VP, Colasson B, Lee LV, et al. In Situ Click Chemistry: Enzyme-Generated Inhibitors of Carbonic Anhydrase II. *Angew Chemie Int Ed*. 2005;44:116–120. https://doi.org/10.1002/anie.200461580.
[23] Morris JC, Chiche J, Grellier C, et al. Targeting Hypoxic Tumor Cell Viability with Carbohydrate-Based Carbonic Anhydrase IX and XII Inhibitors. *J Med Chem*. 2011;54(19):6905–6918. https://doi.org/10.1021/jm200892s.
[24] Wilkinson BL, Bornaghi LF, Houston TA, et al. Carbonic Anhydrase Inhibitors: Inhibition of Isozymes I, II, and IX with Triazole-Linked O -Glycosides of Benzene Sulfonamides. *J Med Chem*. 2007;50:1651–1657. https://doi.org/10.1021/jm061320h.
[25] Wilkinson BL, Innocenti A, Vullo D, Supuran CT, Poulsen S-A. Inhibition of Carbonic Anhydrases with Glycosyltriazole Benzene Sulfonamides. *J Med Chem*. 2008;51(6):1945–1953. https://doi.org/10.1021/jm701426t.
[26] Nocentini A, Ferraroni M, Carta F, et al. Benzenesulfonamides Incorporating Flexible Triazole Moieties Are Highly Effective Carbonic Anhydrase Inhibitors: Synthesis and Kinetic, Crystallographic, Computational, and Intraocular Pressure Lowering Investigations. *J Med Chem*. 2016;59:10692–10704. https://doi.org/10.1021/acs.jmedchem.6b01389.
[27] Pacchiano F, Aggarwal M, Avvaru BS, et al. Selective hydrophobic pocket binding observed within the carbonic anhydrase II active site accommodate different 4-substituted-ureido-benzenesulfonamides and correlate to inhibitor potency. *Chem Commun*. 2010;46:8371. https://doi.org/10.1039/c0cc02707c.
[28] Pałasz A, Cież D. In search of uracil derivatives as bioactive agents. Uracils and fused uracils: Synthesis, biological activity and applications. *Eur J Med Chem*. 2015;97:582–611. https://doi.org/10.1016/j.ejmech.2014.10.008.

[29] Legraverend M, Grierson DS. The purines: Potent and versatile small molecule inhibitors and modulators of key biological targets. *Bioorg Med Chem*. 2006;14: 3987–4006. https://doi.org/10.1016/j.bmc.2005.12.060.

[30] Parker WB. Enzymology of Purine and Pyrimidine Antimetabolites Used in the Treatment of Cancer. *Chem Rev*. 2009;109(7):2880–2893. https://doi.org/10.1021/cr900028p.

[31] Nocentini A, Supuran CT. Carbonic anhydrase inhibitors as antitumor/antimetastatic agents: a patent review (2008–2018). *Expert Opin Ther Pat*. 2018;28 (10):729–740. https://doi.org/10.1080/13543776.2018.1508453.

[32] Raić-Malić S, Svedružić D, Gazivoda T, et al. Synthesis and Antitumor Activities of Novel Pyrimidine Derivatives of 2,3- O, O -Dibenzyl-6-deoxy- l -ascorbic Acid and 4,5-Didehydro-5,6- dideoxy- l -ascorbic Acid. *J Med Chem*. 2000;43:4806–4811. https://doi.org/10.1021/jm0009540.

[33] Manzoor S, Prajapati SK, Majumdar S, et al. Discovery of new phenyl sulfonyl-pyrimidine carboxylate derivatives as the potential multi-target drugs with effective anti-Alzheimer's action: Design, synthesis, crystal structure and in-vitro biological evaluation. *Eur J Med Chem*. 2021;215, 113224. https://doi.org/10.1016/j.ejmech.2021.113224.

[34] Nishimori I, Minakuchi T, Vullo D, Scozzafava A, Innocenti A, Supuran CT. Carbonic Anhydrase Inhibitors. Cloning, Characterization, and Inhibition Studies of a New β-Carbonic Anhydrase from Mycobacterium tuberculosis. *J Med Chem*. 2009;52(9):3116–3120. https://doi.org/10.1021/jm9003126.

[35] Nocentini A, Bua S, Lomelino CL, et al. Discovery of New Sulfonamide Carbonic Anhydrase IX Inhibitors Incorporating Nitrogenous Bases. *ACS Med Chem Lett*. 2017;8(12):1314–1319. https://doi.org/10.1021/acsmedchemlett.7b0039910.1021/acsmedchemlett.7b00399.s001.